PART IX:

HSP

- HSP

Chapter 39
HSP Instrument Overview

In This Chapter...

The High Speed Photometer (HSP) was designed and built at the University of Wisconsin by the HSP Investigation Definition Team (IDT) consisting of Robert C. Bless (Principal Investigator), Joseph F. Dolan, James I. Elliott, Edward L. Robinson, and Wayne van Citters. A general overview of the instrument is given by Bless in "The High Speed Photometer for the Space Telescope," 1982, in *The Space Telescope Observatory*, ed. by D.N.B. Hall, page 106, NASA CP-2244. An instrument closeout summary is provided by Bless et al. in Wisconsin Astrophysics preprint no. 659, 1997.

The HSP was removed from the telescope during the First Servicing Mission in December, 1993 and was replaced by COSTAR.

39.1 HSP Documentation

In this section we list important STScI sources of documentation for the HSP and its various types of output data.

39.1.1 Instrument Handbook

The final version of the *HSP Instrument Handbook* (version 3.0) is a useful description of the technical capabilities of the instrument and practical information for its use.

Although many figures are not currently included, the text of the final version is available in electronic form from the STScI HSP WWW pages. Most earlier versions are now very hard to find and contain little useful information not included in the final version.

39.1.2 Instrument Science Reports

Instrument Science Reports (ISRs) are technical reports issued by STScI that describe calibrations, anomalies, and operational capabilities of the instrument. ISRs are generally written for a technical audience, so we have tried to incorporate their results into this handbook as necessary. When an ISR may be particularly helpful, as in treatment of a topic beyond the scope of this volume, we provide the appropriate reference. Several important ISRs are available electronically on the HSP WWW Documentation page; paper copies of all ISRs are available from the STScI Help Desk; send E-mail to `help@stsci.edu`.

39.1.3 Previous Data Handbooks

This version of the *HST Data Handbook* replaces all previous data handbooks as we have tried to improve upon and slightly expand the treatments in the previous handbooks. Any updates to this handbook will be posted on the STScI WWW site.

39.1.4 HSP WWW Resources

A modest collection of HSP-related documents, including the final *HSP Instrument Handbook*, the IDT SV report, and some of the references listed at the end of Chapter 42 may be found among the STScI World Wide Web resources. The STScI home page is at:

`http://www.stsci.edu/`

The HSP resources can currently be found by looking under “Observing with HST” then “Instruments and Calibration.” Additionally, notices concerning any updates to HSP documentation will be posted here, though none are presently planned.

39.2 Instrument Capabilities and Design

The HSP had five detectors: four image dissector tubes and one photomultiplier tube (PMT). There were two image dissectors with photocathodes sensitive to visual wavelengths (VIS and POL) and two sensitive to the near UV (UV1 and UV2). There were no moving parts in the HSP because the target star was positioned in the desired aperture filter combination (each detector had many filters and apertures) by moving the telescope. A particular aperture was sampled

by the detector *read beam* which was positioned by deflection coils in the detector assembly.

The HSP was designed to obtain high speed photometry with the VIS, UV1, and UV2 detectors in any one of the following modes:

- Single color photometry.
- Star-sky photometry.
- Prism.

The HSP could also be used in the SPLIT mode. In SPLIT mode, simultaneous observations were done using the PMT and the VIS detectors. A complete description of the HSP and its method of operation was given by Bless et al. (1992) as updated by Bless et al. (1997).

The HSP collected two types of data: *digital* and *analog*. Digital data consisted of the count of pulses from a pulse amplitude discriminator for a time equal to the integration time. Analog data was the output of the 12-bit analog-to-digital (A/D) converter. Analog data always produced two bytes of data. There were three science data collection modes:

- Single color photometry.
- Star-sky photometry using one or two detectors.
- Area scans.

Additional detailed information is in the final version of the *HSP Instrument Handbook*.

Chapter 40
HSP Data Structures

In This Chapter...

This chapter contains information about HSP data formats and file types, and necessary reference tables. This chapter does not include a discussion of paper products since no such products exist for the HSP.

40.1 Data Products and File Structures

There are five standard data formats for HSP data. They are listed in Table 40.1.

Table 40.1: HSP Data Formats

Format	Description
BYTE	One-byte digital
WORD	Two-byte digital
LONGWORD (LWRD)	Three-byte digital
ANALOG (ALOG)	12-bit analog (in two bytes)
ALL	Three-byte digital plus two-byte analog

The Post-Observation Data Processing System (PODPS) pipeline calibration process produces datasets in Generic Edited Information Set (GEIS) format. The datasets contain a *standard header packet*, a *unique data log*, and one to four

science data files (and corresponding data quality files). Each file contains an ASCII header file and a binary data file. Each of the files has the same rootname, and the type of file is designated by its suffix. The following table lists the description of the suffixes as determined by the data format and the mode.

Table 40.2: HSP Data Files

Extension	File Contents
Raw Data Files	
`.shh/.shd`	Standard header packet
`.ulh/.uld`	Unique data log
`.d0h/.d0d`	Science data, digital star
`.d1h/.d1d`	Science data, digital sky
`.d2h/.d2d`	Science data, analog star
`.d3h/.d3d`	Science data, analog sky
`.q0h/.q0d`	Data quality, digital star
`.q1h/.q1d`	Data quality, digital sky
`.q2h/.q2d`	Data quality, analog star
`.q3h/.q3d`	Data quality, analog sky
Calibrated Data Files	
`.c0h/.c0d`	Calibrated digital star data
`.c1h/.c1d`	Calibrated digital sky data
`.c2h/.c2d`	Calibrated analog star data
`.c3h/.c3d`	Calibrated analog sky data

40.1.1 Standard Header Packet

The Standard Header Packet (SHP) contains the instrument engineering telemetry values, and other data from spacecraft operations. The telemetry values found in the SHP are observed values and may include quantities that are not controllable.

40.1.2 Unique Data Log

The Unique Data Log contains commanded values for various instrument settings. The UDL also contains data from the flight software.

40.1.3 Science Data Files

Science data are stored as single-precision floating point values. The results of the pipeline calibration are files containing the HSP count rates as a function of time. The number of files in the dataset depends on the mode and the data type. A single observation could generate up to eight separate data files. Science data files are identified by their suffixes as shown in Table 40.2.

40.1.4 Quality Mask Files

Each of the science data files has a corresponding quality file that contains single-precision floating point values. Good data values are identified in the file with a value of zero. An error at any pixel during the data capture process results in a non-zero value. HSP data quality flag values are listed in Table 40.3.

Table 40.3: HSP Data Quality Flag Values

Flag Value	Description
0	Good data
1	Reed-Solomon decoding error
8	A/D converter saturation
16	Missing data

40.1.5 Calibrated Data Files

The HSP calibration program, **calhsp**, generates the calibrated file for each corresponding raw science data file. The calibrated and the raw data header files contain the same keywords, except the raw data are corrected for instrument signatures.

Note that the photometric sensitivity is poorly determined and the calibration correspondingly uncertain.

40.1.6 HSP Data Products

Generally, most HSP data are delivered from the Archive in FITS format. For large volume data samples, FITS format files may not be produced. In this case the delivered data remain in GEIS format.

40.1.7 HSP Keywords

Table 40.4 describes important HSP keywords. This table does not include all keywords that are found in all of the data headers.

Table 40.4: HSP Keywords

Keyword	Description
ROOTNAME	Root file name of the observation dataset
RA_TARG	Right ascension of target, in degrees (J2000)
DEC_TARG	Declination of target, in degrees (J2000)
MODE	Instrument mode (SCP, SSP, or ARS)
DETECTOB	Detector in use (0–5); object data
DETECTSK	Detector in use (0–5); sky data
APERTOBJ	Aperture in use—object data
APERTSKY	Aperture in use—sky data
DEADTIME	Deadtime correction
TRUE_CNT	Compute the true count rates
TRUE_PHC	Compute the true photocurrents
DATA_TYP	Data type (digital or analog)
DATA_SRC	Data source (star, sky, or area scan)
DATA_FMT	Data format (byte, word, lwrd, alog, or all)
TIMEBIAS	Instrument time bias (in seconds)
SAMPTIME	Time of integration (in seconds)
PT_EFFIC	Scaled point source cathode efficiency
EX_EFFIC	Scaled extended source cathode efficiency
DARKRATE	Scaled cathode dark rate
PRE_AMP	Scaled tube pre-amp contribution
HIGHVOLT	Scaled high voltage factor
TUBEGAIN	Scaled tube gain factor
DEADTM	Deadtime
CVCOFSET	Scaled CVC offset
EXPSTART	Exposure start time (modified Julian date)
EXPEND	Exposure end time (modified Julian date)
FILETYPE	shp, udl, or dst (digital sky); dsk (digital sky); ast (analog star); ask (analog sky); asd (area scan digital); or asa (area scan analog)
PTSRCFLG	Point source flag (P for point, or E for extended)

40.2 HSP Reference Tables

Table 40.5 provides a listing of all of the reference tables that are needed for calibration or re-calibration of HSP data. See Chapter 1 for information concerning how to determine the best reference tables and how to retrieve them from the HST Archive.

Table 40.5: HSP Reference Tables in CDBS

Header Keyword for Table	Description
CCP0	Aperture size
CCP1	High voltage factor
CCP2	Gain factor
CCP3	Pre-amplifier noise
CCP4	Relative efficiency
CCP5	Dark signal
CCP7	CVC offset
CCP8	Dead time
CCP9	Dark aperture name

40.3 Displaying HSP Data

To get started using IRAF and STSDAS refer to the tutorial information in Appendix A of Volume I of this manual, or in the *STSDAS Users Guide*. An example of displaying HSP data is provided below.

40.3.1 Displaying the SHP and UDL

The header consists of engineering telemetry values, plus other information. The SHP and the UDL each contain two groups. This should be checked by looking at the keyword GCOUNT. The value for GCOUNT should be 2. The keyword PTSRCFLG (point source flag) should list either P for a point source or E for an extended source. The IRAF task **listpixels** under the **images** package can be used to look at the values of the SHP and UDL pixels. The following chart

shows the correct value for SHP pixel #937 according to MODE and if the source is EXTENDED or POINT.

Table 40.6: Correct Value for SHP Pixel Value 937

Mode	Source	SHP 937 Pixel Value
SCP	P	1
SSP	P	2
SCP	E	257
SSP	E	258
ARS	–	3

40.3.2 Displaying HSP Area Scans

HSP area scans can be displayed by using the IRAF **surface** or **contour** tasks under the **plot** package.

You can display area scans (which make little images) using the IRAF **display** task and SAOimage, described on page 3-4. The time series data can be displayed using either **splot** (page 3-25) or **implot** (page 3-10), which will make one-dimensional plots of counts versus time.

Figure 40.1: HSP Area Mode Display

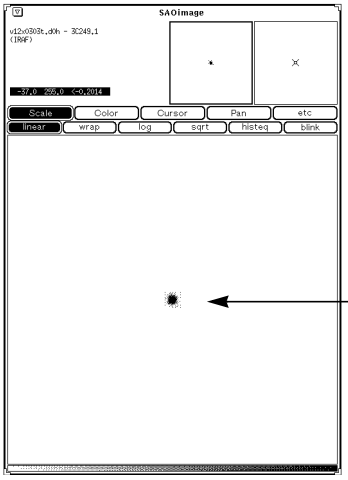

Figure 40.2: HSP Time Series Data Plot

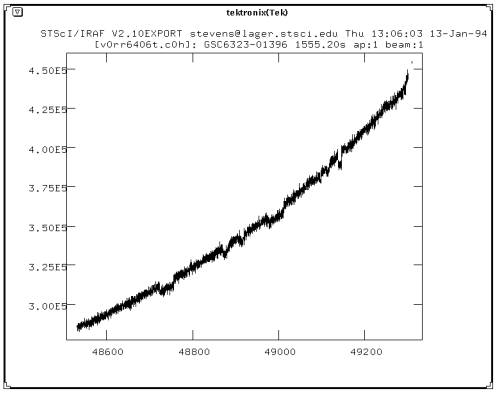

Chapter 41
Calibrating HSP Data

In This Chapter...

This chapter explains how HSP data are calibrated. Discussions include information about the data format and file types, details about the calibration pipeline, its keyword switches, and necessary reference tables.

41.1 Pipeline Calibration

The HSP pipeline reduction was not used extensively by the HSP team, for a number of reasons. For example, many datasets are too large for IRAF and the ground system simply could not produce a FITS file. Some HSP data were taken at such high speeds that the time series consist of a few ones separated by large runs of zeroes, making the deadtime corrections and dark count subtraction inappropriate. Other calibrations, such as absolute timing of data samples, required working with fundamental data such as daily spacecraft clock calibrations which were not available to the pipeline as quickly as needed.

For these and other reasons, most HSP datasets were reduced in-house at the University of Wisconsin when needed. The following description of the pipeline will give the user an introduction on how raw data are converted into calibrated data.

HSP data are received in the raw and calibrated format. The STSDAS **calhsp** task can be run to recalibrate the raw HSP data. **calhsp** takes the raw GEIS files containing counts in the digital data and digital numbers in the analog data and

converts the data to calibrated data containing counts per second for point source and counts per second per square arcsecond for extended source data. All of the various data formats get calibrated, except for area scan data.

The **calhsp** task performs the following basic calibration processing steps (note that the sequence differs somewhat depending on the data type, see the flowchart on the next page):

- If the data are digital, raw data will be converted to count rate before any corrections are performed.
- Subtract detector dark background.
- Subtract pre-amplifier noise.
- Correct for high voltage factor.
- Correct for relative sensitivity.
- Correct analog data for gain factor (at this step, the DN reading is converted to counts per second).
- Subtract current-to-voltage converter offset from analog data.
- Subtract non-linearity caused by dead time in digital data.
- Convert raw data to count rate.
- For extended targets, divide count rates by the aperture area.

41.2 Calibration Switches

The HSP has three calibration switches: DEADTIME, TRUE_CNT, and TRUE_PHC. The first two apply to digital data, and the third applies to analog data. The calibration switches can be either turned on (set to PERFORM) or turned off (set to OMIT). Digital and analog data are calibrated differently. Digital data can be calibrated by: full calibration (both switches on), deadtime calibration (DEADTIME switch only), true count calibration (TRUE_CNT switch only), and no calibration (both switches off). Because an analog dataset has only one switch, the data are either calibrated or not calibrated. The switches were turned on or off during the reformatting in PODPS.

The following table lists the calibration switches currently used.

Table 41.1: HSP Calibration Switches

Switch	Description
DEADTIME	Correct dead time
TRUE_CNT	Compute true count rates for digital data
TRUE_PHC	Compute true count rates for analog data

Figure 41.1: Pipeline Processing by calhsp

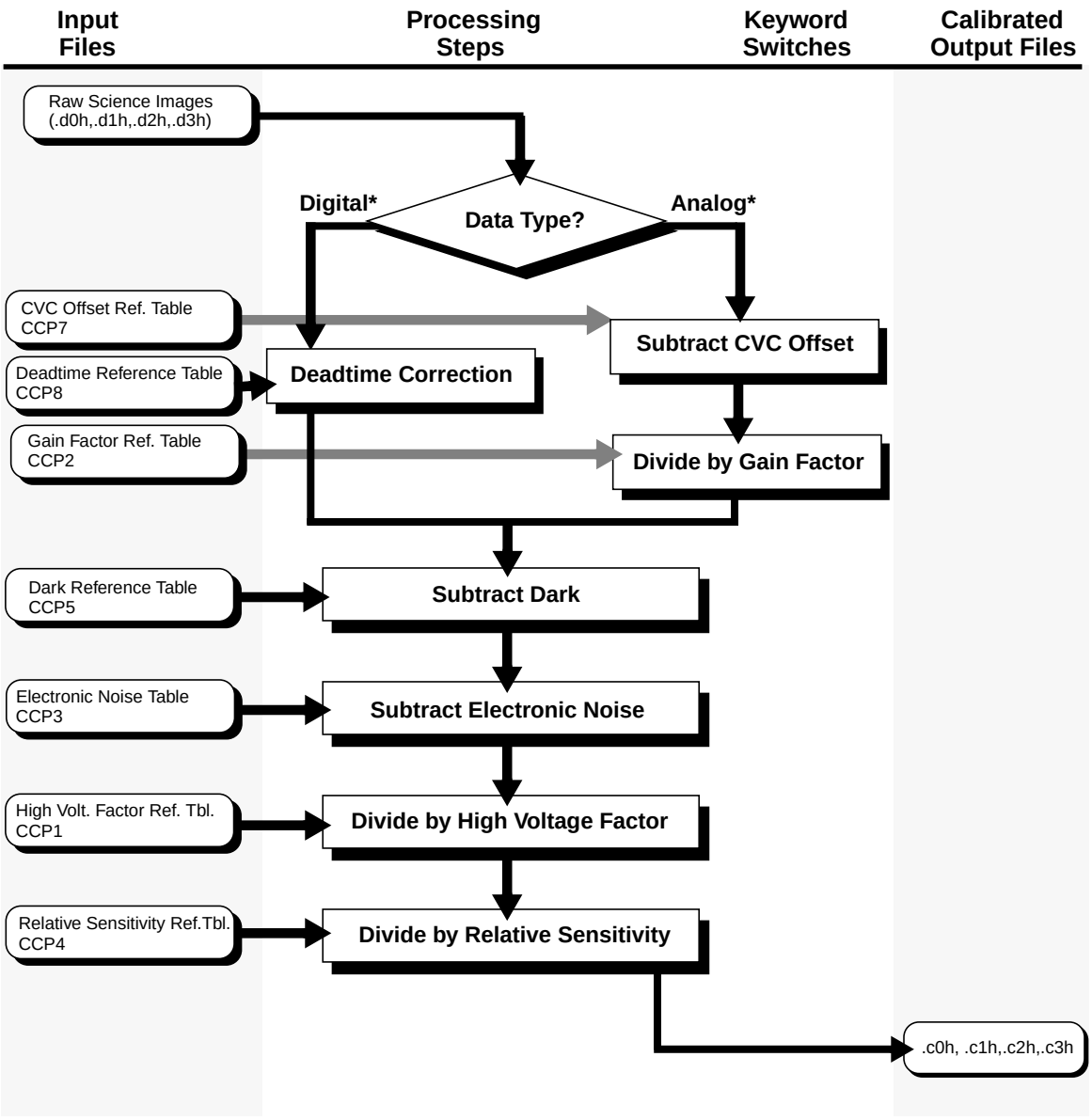

* All **analog** steps are performed when the TRUE_PHC switch is turned on.
For **digital** data, dead time correction is turned on using the DEADTIME switch, and all other steps are turned on using the TRUE_PHC switch.

41.3 Calibration Algorithms

Here we describe the algorithms used for each of the calibration steps:

- Correcting for dead time.
- Computing the true count rates for digital data.
- Computing the true count rates for analog data.

41.3.1 Correcting for Dead Time

The raw counts need to be converted into count rate. The following equation is used to find the count rate.

$$x = (raw\ counts / sample\ time)$$

Where x is the observed count rate.

The following equation is used to correct for dead time.

$$y = x / (1 - x\ t)$$

Where:

- y – is the true count rate after deadtime correction.
- x – is the observed count rate.
- t – is the dead time.

41.3.2 Computing the True Count Rate

True count rates for digital data are corrected by using the first equation for a point source and the second for an extended source.

$$a = (y - pre\_amp - darkrate) / (highvolt \times pt\_effic)$$

$$b = \frac{(y - pre\_amp - darkrate) / (highvolt \times ex\_effic)}{aperarea}$$

Where:

- a – is the final calibrated true count rate for point source.
- b – is the final calibrated true count rate for extended source.
- y – is the true count rate after deadtime correction.

41.3.3 Computing the True Photocurrents

True photocurrents (count rates for analog data) are corrected by the first equation for point sources and the second equation for extended sources.

$$c = \frac{[(n - cvc\_offset)/tubegain] - (darkrate + pre\_amp)}{highvolt \times pt\_effic}$$

$$d = \frac{[(n - cvc\_offset)/tubegain] - (darkrate + pre\_amp)}{highvolt \times ex\_effic \times aperarea}$$

Where:

- *c* – is the final calibrated true count rate for point source.
- *d* – is the final calibrated true count rate for extended source.
- *n* – is the observed digital number.

41.3.4 Calculating Sample Time

The following equation is used to calculate the sample time. The sample time can be found in the data headers under the keyword SAMPTIME.

$$samptime = \frac{int\_time + timebias}{1.024 \times 10^6}$$

41.3.5 Calibration Parameter Polynomial

The HSP calibration parameters listed in Table 41.2 are calculated using the following polynomials.

$$X = X0 * [1.0 + a01 * (t - t0) + a02 * (t - t0)^2 + a03 * (t - t0)^3]$$
$$+ [a10 + a11 * (t - t0) + a12 * (t - t0)^2 + a13 * (t - t0)^3] * (T - T0)$$
$$+ [a20 + a21 * (t - t0) + a22 * (t - t0)^2 + a23 * (t - t0)^3] * (T - T0)^2$$
$$+ [a30 + a31 * (t - t0) + a32 * (t - t0)^2 + a33 * (t - t0)^3] * (T - T0)^3$$

Where:

- *X* – is the calibration parameter value.
- *X0* – is the base value of the calibration parameter.
- *t* – is the epoch (time in modified Julian days) of the observation.
- *t0* – is the base time.
- *T* – is the temperature.
- *T0* – is the base temperature.

Table 41.2: HSP Calibration Polynomials

Parameter	Definition
pre_amp	Scaled tube pre-amp contribution
darkrate	Scaled cathode dark rate
highvolt	Scaled high voltage factor
pt_effic	Scaled point source cathode efficiency
ex_effic	Scaled extended source cathode efficiency
cvc_offset	Current-to-voltage converter offset
tubegain	Scaled tube gain factor

41.4 HSP Calibration Parameter Tables

Table 41.3 lists the HSP calibration parameters as found in the Calibration Data Base (CDBS). When using **calhsp**, CDBS values are read into STSDAS binary tables. The tables are required in order to run a complete calibration of the data. These tables are all stored in the HST Archive and can be retrieved from there as described in Chapter 1.

Table 41.3: HSP Reference Tables in CDBS

Relation	Header Keyword	Description
cvccp0r	CCP0	Aperture size
cvccp1r	CCP1	High voltage factor
cvccp2r	CCP2	Gain factor
cvccp3r	CCP3	Pre-amplifier noise
cvccp4r	CCP4	Relative efficiency
cvccp5r	CCP5	Dark signal
cvccp7r	CCP7	CVC offset
cvccp8r	CCP8	Dead time
cvccp9r	CCP9	Dark aperture name

Chapter 42
HSP Error Sources and Data Analysis

In This Chapter...

In this chapter we provide details concerning the accuracies and contributing error sources for a variety of HSP modes, instrumental characteristics, and calibrations. The last section of the chapter presents a bibliography of useful HSP publications referenced in this handbook.

42.1 Uncertainty in EXPSTART and EXPEND

An uncertainty of ~0.1 seconds was found in the way in which EXPSTART and EXPEND are calculated. The time indicated in the FITS headers for these keywords is only accurate to 1 second. *HSP ISR 12* (Percival, 1992) describes in detail the reduction of the five HSP observations of the Crab pulsar [reference 2]. In that document, a detailed description of the correlation of the HST clock with UTC is defined.

42.2 Disagreement Between PTSRCFLG and SHP

During early HSP activities, the HSP keyword PTSRCFLG was found to be in disagreement with the SHP pixel value. The FITS header states PTSRCFLG as an extended source, whereas the SHP pixel value 937 lists it as a point source. The problem was caused in proposal transformation.

42.3 Correcting Times in PRISM and STAR-SKY Modes

In the PRISM and STAR-SKY modes, the read-beam had to be moved back and forth between different filter-aperture pairs. The data stream that is produced by the pipeline alternates between filter 1 and filter 2 or between star and sky. The actual *relative* times of each observation must be adjusted to account for the time required to move the read-beam between successive observations. This delay time, *N*, is a function of data format and can be computed from Table 42.1 below, which specifies *N* in units of 1/1,024,000 second for each data format and which gives the approximate corresponding delay time in msec, as well.

Table 42.1: Delay Time as a Function of Data Format

Data Format	Delay TIme (*N*)	Delay Time (msec)
BYTE	20,075	19.60
WORD	20,099	19.63
LONGWORD (LWRD)	20,119	19.65
ANALOG (ALOG)	20,300	19.82
ALL	20,157	19.68

42.4 Prism Aperture Calibration

The HSP prism mode split the light from a single target into two separate apertures on adjacent filters. By moving the read beam, the light through the two aperture-filter pairs was alternately observed. The initial post-launch verification tests produced unexpectedly low transmission results. Other HSP tests to calibrate the prism apertures were run, but showed the throughput to be lower than expected. The current estimate is a lower throughput of 3–4 magnitudes.

Due to small misalignments of the beam splitter prisms, PRISM mode was even more highly susceptible to the effects of telescope jitter than normal one-color photometry.

Table 42.2 summarizes the throughput of the prism apertures relative to pre-flight calibrations.

Table 42.2: Throughput of Prism Apertures

Filter/Detector	λ_{eff} (Å)	Loss Factor
F248/UV1	2462	9.5
F135/UV1	1549	6.0
F262/UV2	2606	7.0
F145/UV2	1556	8.8
F551/VIS	5482	20.4
F240/VIS	2192	3.9

42.5 VIS Degradation

The HSP experienced a loss in sensitivity in the visual (VIS) detector over much of the period of operation. Analysis has shown no evidence in telemetry to suggest an electronic failure in the VIS detector.[3]

The degradation was found by measuring the flux of the star through the finding aperture (VCLRV_T). Two separate targets, VID998 and BD+75D325, were used as photometric standards. The accuracy of the flux calibrations was at the level of photon counting statistics or better for the test. The VIS tube has decreased by about a factor of 3.2 from April 1991 through August 1993, but the final calibrations between October and December of 1993 showed a return to levels typical of the beginning of calibrations in April 1991. This level held through several calibrations including the last taken on the final day of HSP operations. Figure 42.1 shows the VIS flux from observations of VID998 and BD+75D325 over this period. The other detectors showed no change in flux measurements over time.

The UV1, UV2, and POL detector sensitivities were all constant within 1% over the same time period.

Figure 42.1: VIS Degradation

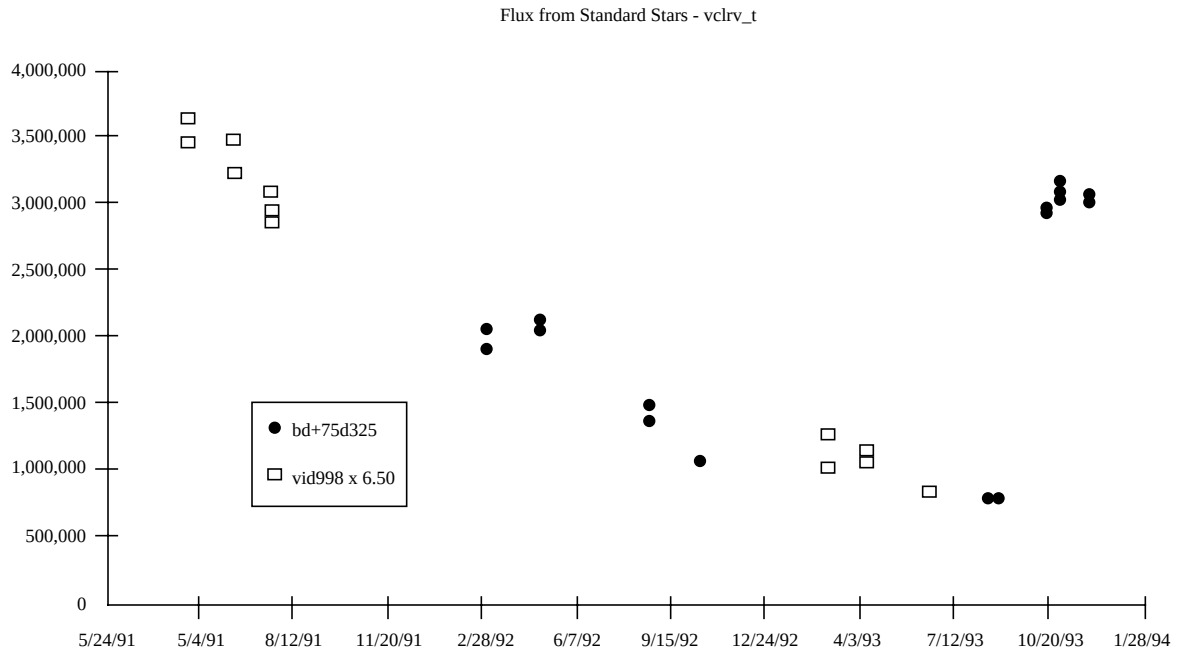

42.6 Orbital Period and Ramp

A science verification test to check the short term photometric stability of the HSP was run in August 1991. The rapidly oscillating Ap star HD60435 was chosen because of its position in a region of the sky that was continuously visible from HST and also its intrinsic variabilities were well known. Data was collected for 5.5 hours. Figure 42.2 is a plot of the data obtained from the test. The data shows two unexpected effects: a sinusoidal oscillation with a 94-minute period and a monotonic increase in flux. Both the zero-to-peak amplitude of the 94 minute oscillation and the total amplitude of the monotonic linear ramp are about one percent.

Figure 42.2: 1389 SCP Data

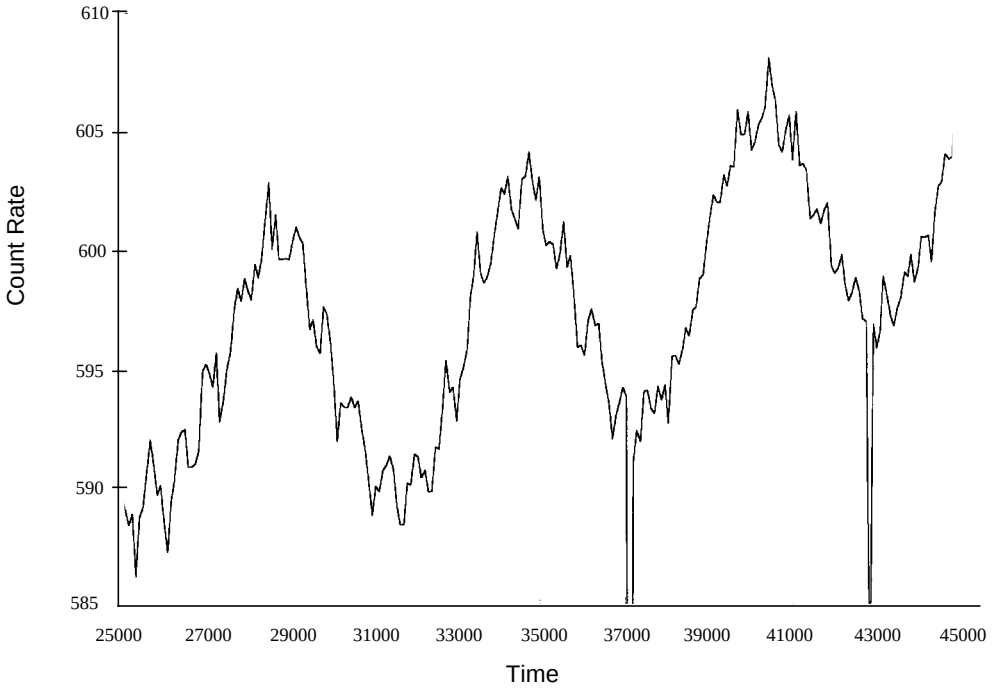

Nelson [5] states that these sinusoidal variations occurred in all HSP data. Several tests to understand these photometric changes were preformed with the HSP and other HST instruments. Onboard temperatures exhibited a sinusoidal variation with a period equal to the orbital period of the telescope but a causal relationship between the temperature of a particular location on the telescope and the photometry has not been established.

An orbital periodic axial motion of the focal plane known as *breathing* has been acknowledged[6]. Nelson has used models of the HST PSF at the HSP position in the focal plane to determine that the 2.5% variation (peak to peak) as seen in the 1389 data, would take 8 to 10 microns (peak to peak) of axial motion of the secondary mirror (despace).

A test run by STScI resulted in an empirical formula using OTA temperatures that corresponds to the orbital period and ramp of the HSP data [7], but a correction to the data has not been defined.

The HSP team has been able to fit these systematic variations with an equation that models the fluctuations well and can be used to correct the data to within photon statistics. However, this is done at the expense of eliminating any possible detection of intrinsic variability which occurs on the timescales of these systematic fluctuations.

42.7 SDF Clock Errors

HSP has encountered several error reports which seem to indicate that the HSP line counts were out of order. Actually, however, the line counts were in order and the time annotation of the line start by the Control & Data Handler (C&DH) appears to be incorrect. This problem appears to have two signatures. One is that the clock insertion into the packet seems to be interrupted such that the second word of the clock is set prior to an update and the low order clock value after a 125 millisecond step. The second signature is that the C&DH maintained clock value seems to have counted more than 60 seconds of vehicle counts.

The problem can be detected by looking at the packet sequence. Sorting by packet count gives a time-tag inversion, sorting by SDF packet time, gives a line count inversion. Figure 42.3 is an excerpt from a listing of packet headers. The time column is in seconds, the delta is the delta-time from the previous packet. Packet 4112 comes before 4111, and the delta-time is 0.000977 seconds, which is exactly 1000 clock ticks at 1.024 MHz.

Figure 42.3: Listing of Packet Headers

pkx	obs	owner	pfc	spp	wpp	ppf	fcount	lcount	time	delta
1	39	HSP	0140	1	34	52941	19	4099	90919501.904297	0.000000
2	39	HSP	0140	1	34	52941	19	4100	90919501.913086	0.008789
3	39	HSP	0140	1	34	52941	19	4101	90919501.921143	0.008057
4	39	HSP	0140	1	34	52941	19	4102	90919501.929932	0.008789
5	39	HSP	0140	1	34	52941	19	4103	90919501.938232	0.008301
6	39	HSP	0140	1	34	52941	19	4104	90919501.947144	0.008911
7	39	HSP	0140	1	34	52941	19	4105	90919501.955200	0.008057
8	39	HSP	0140	1	34	52941	19	4106	90919501.964111	0.008911
9	39	HSP	0140	1	34	52941	19	4107	90919501.972168	0.008057
10	39	HSP	0140	1	34	52941	19	4108	90919501.981201	0.009033
11	39	HSP	0140	1	34	52941	19	4109	90919501.989258	0.008057
12	39	HSP	0140	1	34	52941	19	4110	90919501.998901	0.009644
13	39	HSP	0140	1	34	52941	19	4112	90919502.005371	0.006470
14	39	HSP	0140	1	34	52941	19	4111	90919502.006348	0.000977
15	39	HSP	0140	1	34	52941	19	4113	90919502.013672	0.007324
16	39	HSP	0140	1	34	52941	19	4114	90919502.023315	0.009644
17	39	HSP	0140	1	34	52941	19	4115	90919502.030762	0.007446
18	39	HSP	0140	1	34	52941	19	4116	90919502.039307	0.008545
19	39	HSP	0140	1	34	52941	19	4117	90919502.047852	0.008545
20	39	HSP	0140	1	34	52941	19	4118	90919502.056396	0.008545
21	39	HSP	0140	1	34	52941	19	4119	90919502.064697	0.008301

There is no conclusive proof as to the frequency or randomness of these signatures. The HSP team has requested a change in the sort order to specify lines first and time second when processing the data.

42.8 Bogus Data Packets

Some HSP data were corrupted by bad data packets. The bad packet consists of 1930 bytes, alternating in value between 1 and 0. This replacement affected 0.0016% of the samples in a dataset, but accounted for 0.4% of the total counts, subtly affecting the statistics. The false data were injected at precisely the Nyquist frequency, helping to hide its effect in the Fourier domain. We stumbled onto this by performing statistical analysis on the raw Science Data Formatter (SDF) packets, not typically provided to users. The packets were corrupted onboard the HST, but after the data left the HSP. Several things point to this.

- First, normal HSP packets have 1920 bytes of data, and the C&DH adds 10 bytes of fill data to round out the segment. In the corrupted packets, the fill bytes are absent. The fact that the non-HSP portions of the packet are affected makes it unlikely that the HSP is the cause.
- Second, the “Mission ID” field, which normally holds a value of 58, has a value of zero in the bad packets. This would imply some problem in the C&DH packet handling.
- Third, the C&DH time stamps in the packet headers show some unusual timing. Packets are collected at the expected rate, but then a double packet time elapses, followed by two packets in quick succession. The bad packet is the second of this pair.

42.9 Data Echo Problem

There is a significant undiagnosed problem that can occur in time series datasets. On two different occasions, autocorrelation analyses revealed an unexpected spike of power at lags of 8.6 ms and 9.4 ms, respectively. This turned out to be caused by small patches of time series data being copied from one part of the dataset to another.

The data were organized in packets inside the HSP, and were treated as packets all the way through the system until the HST ground system at STScI reformatted them into a simple time series. The HSP team discovered that data from the beginning of packet 7 were appearing at the beginning of packet 8, and similarly for packet pairs 15 and 16, 23 and 24, and so on. The packet collection times in these two isolated instances were 8.6 ms and 9.4 ms, accounting for the results in the autocorrelation. The length of the duplicated stretch varied randomly from 12 to 24 samples.

Extensive analyses were performed by the HSP team and by experts in the operation of the Science Data Formatter (SDF), the packet interface to which the HSP sends data. No likely suspects were found. A simple “numerological” analysis also failed to implicate or exonerate any specific subsystem. For example, the HSP maintains 8 internal packet buffers, easily raising eyebrows with the period-of-8 repetition reclamation error affecting pairs of packets. That is, packets

0 and 8 shared buffers, not 7 and 8. On the other hand, packets appeared pairwise in the SDF, which maintained two ping-pong packet buffers. The SDF could generate defective packet time stamps, which then caused the ground system to put packets in the wrong order, although this was not expected to change the contents of a packet.

This autocorrelation test was performed on many datasets taken with precisely the same instrument configuration, with no irregularities found. Only four datasets (taken on 2 days less than 1 week apart) have been discovered to show this effect. *If you have data taken at sample rates exceeding 1 kHz, do an autocorrelation and look for spurious power at lags equal to a packet collection time, which is the sample time multiplied by the number of samples per packet.* The latter value is given in the SMS command load or in the FITS headers for the data.

42.10 Expected Accuracies of HSP Data

HSP photometric accuracies are strongly dependent on the observational setup and observing conditions, such as spacecraft jitter. Absolute photometry can be done only with a one sigma limiting accuracy of approximately 5%, but relative photometry is possible with an accuracy of 1–2%.

Table 42.3: Estimated HSP Calibration Accuracies

Attribute	Estimated Accuracy	Comments
Absolute Timing	~10 millisec	Can be achieved from science headers if HST/UTC timing regression coefficients appropriate to observation date were used in post-observation calibration; otherwise, use methods from *HSP ISR 12*.
Relative Timing (timing resolution)	Digital modes: 10.7 microsec Analog modes: ~1 millisec	For PRISM mode: relative timing given by science headers must be corrected for format-dependent read-beam switching time (see page 42-2).
Detector stability:	Sensitivity: UV1, UV2, POL all constant within 1%; VIS: factor of 3 decrease then recovery	1991 through summer 1993 monotonic decrease, post-August 1993 complete recovery
Detector linearity:	linearity: +/- 0.01 mag	VIS 551W for magnitude range 5.11 < V < 12.79
Absolute photometry (flux calibration)	5% (one sigma)	Limited by breathing effects and small differences in telescope pointing at different standard star observing epochs
Relative photometry	1-2%	Limited by guiding, re-acquisition centering, orbital effects (breathing, jitter)
Polarimetry: q,u,p	0.3% (one sigma) F327M and F277M	Add in quadrature with photon statistical uncertainty
Aperture Location	Absolute: <50 milliarcsec Relative: <20 milliarcsec	

42.11 Further Analysis

The following types of analysis are described in other documents. References are listed in the next section. Some of these documents are available through the STScI HSP WWW site.

- Detecting periodicities in HSP data. [9]
- Removing effects from HST and not from the HSP or any intrinsic variability of the target. [9] An empirical model, when applied to the raw data, restores a constant source to a constant photometric output.
- Detecting pulsars in HSP data. [10]
- HSP pulsar timing and light curve reduction. [2]
- Analysis of occultation data using the HSP. [11]
- Polarization results from the HSP. [12]
- Spherical aberration and how it affects the HSP. [12]
- Photometry of the HSP and overall reliability. [12]

42.12 References

1. Bless, R.C., Percival, J.W., Walter, L.E., White, R.L. 1992, *High Speed Photometer Instrument Handbook.*

2. Percival, J.W., "High Speed Photometer Pulsar Timing and Light Curve Reduction", *HSP Instrument Science Report* #12, 1992

3. Townsley, L.C. "Investigation of HSP VIS Loss in Sensitivity", *HSP Instrument Science Report*, 1993, October 1993.

4. Richards, E.E., Percival, J.W., Nelson, M.J., Townsley, L.C., Hatter, E. "Operations Experiences of the Space Telescope High Speed Photometer", SPIE VOL Space Astronomical Telescopes and Instruments, 1993.

5. Nelson, M.J., "Orbital Periodic Errors in HSP Photometry," *HSP Instrument Science Report* #15, December 1992.

6. Bely, P.Y., and H. Hasan, "Estimate of the Tolerance on Short Term Focus Change (Breathing Effect)," OTA Science Report #11, 1989.

7. Bely, P.Y. "Preliminary Analysis of the Breathing Test", June 2, 1993.

8. *STSDAS User's Guide*, 1994.

9. Taylor, M.J., Nelson, M.J., Bless, R.C., Dolan, J.F., Elliot, J.L., Percival, J.W., Robinson, E.L., Van Citters, G.W., "High Speed Ultraviolet Photometry of HD60435", *Ap.J.*, 413, L125, 1993.

10. Percival, J.W., Biggs, J.D., Dolan, J.F., Robinson, E.L., Taylor, M.J., Bless, R.C., Elliot, J.L., Nelson, M.J., Ramseyer, T.F., Van Citters, G.W., Zhang, E., "The Crab Pulsar in the Visible and Ultraviolet with 20 Microsecond Effective Time Resolution", 1993, *Ap.J.*, 407

11. Elliot, J.L., Bosh, A.S., Cooke, M.L., Bless, R.C., Nelson, M.J., Percival, J.W., Taylor, M.J., Dolan, J.F., Robinson, E.L., and Van Citters, G.W., "An Occultation by Saturn's Rings on 1991 October 2-3 Observed with the Hubble Space Telescope", *AJ*, 106, 2544.

12. Bless, R.C., Richards, E.E., Dolan, J.F., Elliott, J.L., Nelson, M.J., Percival, J.W., Robinson, E.L., Taylor, M.J., Van Citters, G.W., and White, R.L., "The Hubble Space Telescope High Speed Photometer", 1997, University of Wisconsin Astrophysics No. 659.